This is the accepted manuscript version of the contribution published as:

Drechsler, M. (2023):

Ising models to study effects of risk aversion in socially interacting individuals *Physica A* **632**, **Part 1**, art. 129345

The publisher's version is available at:

https://doi.org/10.1016/j.physa.2023.129345

Ising models to study effects of risk aversion in socially interacting individuals

Martin Drechsler, Helmholtz Centre for Environmental Research – UFZ, Permoserstr. 15, 04318 Leipzig, Germany; and Brandenburg University of Technology Cottbus-Senftenberg, Cottbus, Germany; martin.drechsler@ufz.de.

Abstract

10

15

20

25

Ising models have been applied not only to describe physical systems but also systems of interacting animals and humans. In contrast to physical entities, animal and humans exhibit more complex behaviour such as risk aversion, so that certain payoffs are, for given expected payoff, preferred to uncertain payoffs. Here I extend the classical Ising model to consider of risk aversion, and show that this affects the model's stability domains: if individuals are risk averse and their choices differ by the associated risk levels, then higher coupling constants are required to sustain system states in which the riskier choice is abundant; otherwise the risky choice is accompanied (bistability) or even replaced in the system by the less risky choice. The model and results are applied to an economic incentive scheme for the conservation of biodiversity, the agglomeration bonus, that induces not only conservation measures but rewards their spatial agglomeration. Here conservation is the risky choice whose abundance in the land-use system is shown to decline if the landowners are risk-averse.

Key words

agglomeration bonus, biodiversity conservation, Ising model, risk aversion.

Highlights

Risk aversion is included in the classical Ising model

Risk aversion affects the stability domains of the model

The agglomeration bonus incentivises spatially aggregated biodiversity conservation

30 Risk-averse landowners under an agglomeration bonus conserve less land

1 Introduction

35

40

45

50

55

After its introduction by Ernst Ising for the description of phase transitions in ferromagnets, the Ising model has been applied to many systems in and outside physics. Physical applications include, among others, spin glasses [1](Fischer and Hertz 1991) and ice-water phase transitions [2](Ma and Sudakov 2017). Closely related are neural networks and applications in the field of computer-based learning and pattern recognition [3–5](Jaynes 1957, Derrida et al. 1987, Krasnytska et al. 2021).Biological applications consider, e.g., cooperation among bacteria [6–7](Shi and Duke 1998, Bai et al. 2010) genetics [8] (Majewksi 2001).

Its focus on the interaction between entities makes the Ising model especially suitable for the study of social phenomena. Examples from human societies include social polarisation [9] (Schelling 1969), language change [10] (Stauffer 2008) and the formation and spread of opinions [11, 12] (Grabowski and Kosiński 2006, Garrod and Jones 2021), as well as the dynamics of stock markets [13] (Valle et al. 2021). In addition, Ising models have been used to model social interactions among animals [14–16] (Battacharya and Vicsek 2010, Wilson 2017, Lecheval et al. 2018).

Relative to physical and simple biological entities, humans and many animals show more complex decision behaviour. An important one is risk aversion. Spins, in their alignment, follow the simple "objective" of minimising their free energy, which in the context of human behaviour means that some expected payoff is maximised. Such behaviour that disregards uncertainties in the payoff is termed "risk-neutrality". In humans it is rather the exception in humans who are generally risk-averse – aiming, next to the maximisation of expected payoffs, at the minimisation of the risk of low payoffs [17, 18](Eeckhoud et al. 2005, Chen 2016). Often there is a trade-off between the two objective (as, e.g., in finance), so that for a higher expected payoff a higher risk must be accepted. Risk aversion is observed not only in humans but also in animals like lizards [19] (Batabyal et al. 2017), rats [20] (Constantinople et al. 2019), coral-reef fishes [21] (Coni et al. 2021), pigeons [22] (Clayton et al. 2022) and chimpanzees [23] (Haux et al. (2023).

60

65

Here I extend the classical Ising model developed for the ferromagnet to study effects of risk aversion in a model society of interacting individuals. After the analysis of the general model I consider an application recently presented by Drechsler (2023) [24] who analysed the agglomeration bonus for the conservation of biodiversity by Parkhurst et al. (2002) [25]. The analysis was motivated by the fact that on private lands, biodiversity conservation measures are usually implemented through spatially homogenous conservation payment schemes to offset the profit losses and other costs incurred by conservation measures. To control not only for the amount

but also the spatial allocation of conservation efforts (to counter the continuing fragmentation of species habitats), coordination incentives have been proposed [26] (Nguyen et al. 2022).

The most popular and most frequently studied example is that agglomeration bonus [24, 26] (Nguyen et al. (2022) and Drechsler (2023) in which the spatially homogenous base payment is accompanied by a bonus for each adjacent land parcel that is conserved, too. Here I analyse how the introduction of risk aversion changes the land use induced by the agglomeration bonus. Both in the general analysis and the application, risk aversion reduces the abundance of the riskier choice in the model system which either becomes bistable or is dominated by the less risky choice.

2 Ising model with risk aversion

2.1 Methods

70

75

95

Following Phan et al. (2003) [27], a society of individuals i (i = 1, ..., N) is considered, each with the choice between two actions $s_i \in \{-1,+1\}$ that lead to the individual's benefits

$$V_i(s_i) = (h + \sigma \varepsilon_i) s_i + \frac{J}{L} s_i \sum_{j \in L_i} s_j$$
(1)

Here ε_i is a random number with mean zero and standard deviation one, so that hs_i and σ are the mean and standard deviation of the normal distributed individual's idiosyncratic benefit for chosen s_i. The term with s_iΣs_j describes the interaction of individual i with the individuals in its neighbourhood L_i. The number of individuals in this neighbourhood is assumed the same for all individuals and equal to L. Parameter J/L measures the influence of each neighbour on the benefit of individual i. In the ferromagnet, s_i would be the spins, h the external field and J/L the coupling constant.

Now I introduce an asymmetry in the interaction, so that J is a function of s_i (if s_i represents, e.g., the choice of a smartphone \in {iphone, Samsung} this would mean that the decision to purchase an iphone might be more strongly influenced by the peers' choices than the decision to purchase a Samsung phone). Formally, I assume that $J(s_i) = J_0 + s_i \Delta$, so eq. (1) becomes

$$V_i(s_i) = (h + \sigma \varepsilon_i) s_i + \frac{J_0 + s_i \Delta}{L} s_i \sum_{j \in L_i} s_j$$
(2)

Like Phan et al. (2003) [27] I consider that the sizes of the s_j are not known to individual i, so the benefit V_i is uncertain with expectation value $E_j[V_i]$. The subscript i is suppressed here for simplicity, and the subscript j indicates that E[] is evaluated as a function of the j contained in neighbourhood L_i . In addition to Phan et al. (2003) [27] I also consider the variance of the benefit, $\text{var}_j[V_i]$.

105

The risk attitude of the individuals is considered by assuming that they maximise the risk-utility function

$$U_{i}(s_{i}) = E_{j}[V_{i}(s_{i})] - \rho \operatorname{var}_{j}[V_{i}(s_{i})],$$
(3)

110

where $\rho > 0$ models risk aversion, $\rho = 0$ risk neutrality, and $\rho < 0$ models risk-loving behaviour [28] (Nakamura 2015). This function explicitly considers the trade-off between expected payoff and risk mentioned above. For the expectation $E_i[V_i]$ we have

$$E_{j}[V_{i}(s_{i})] = (h + \sigma \varepsilon_{i})s_{i} + (J_{0} + s_{i}\Delta)s_{i}E_{j}[s_{j}]$$

$$(4)$$

and the variance equals

$$\operatorname{var}_{j}[V_{i}(s_{i})] = E_{j}[V_{i}^{2}(s_{i})] - E_{j}[V_{i}(s_{i})]^{2}.$$
(5)

120

The first term on the right-hand side, the expectation value of $V_i^2(s_i)$, equals

$$E_{j}[V_{i}(s_{i})^{2}] = (h + \sigma\varepsilon_{i})^{2} + 2(h + \sigma\varepsilon_{i})(J_{0} + s_{i}\Delta)E_{j}[s_{j}] + \left(\frac{J_{0} + s_{i}\Delta}{L}\right)^{2}E_{j}\left[\left(\sum_{j \in L_{i}} s_{j}\right)^{2}\right], \tag{6}$$

and the second term, the square of the expectation value, equals

$$E_{j}[V_{i}(s_{i})]^{2} = (h + \sigma\varepsilon_{i})^{2} + 2(h + \sigma\varepsilon_{i})(J_{0} + s_{i}\Delta)E_{j}[s_{j}] + \left(\frac{J_{0} + s_{i}\Delta}{L}\right)^{2}E_{j}\left[\sum_{j\in L_{i}}s_{j}\right]^{2},$$
(7)

so the variance of the benefit is

$$\operatorname{var}_{j}[V_{i}(s_{i})] = \left(\frac{J + s_{i}\Delta}{L}\right)^{2} \left[E_{j}\left[\left(\sum_{j \in L_{i}} s_{j}\right)^{2}\right] - E_{j}\left[\sum_{j \in L_{i}} s_{j}\right]^{2}\right] = \left(\frac{J + s_{i}\Delta}{L}\right)^{2} \operatorname{var}_{j}\left[\sum_{j \in L_{i}} s_{j}\right]. \tag{8}$$

Here the role of Δ becomes visible. For $\Delta > 0$ the variance $\text{var}_j[\Sigma s_j]$ of the neighbouring spins is weighted more strongly if $s_i = +1$ than if $s_i = -1$ (for $\Delta < 0$ the opposite is valid). Parameter Δ thus measures the difference between the risks associated with the two choices $s_i = +1$ and -1.

For evaluate the variance $\operatorname{var}_{j}[\Sigma_{j}s_{j}]$ in closed form, I consider that the number n_{j}^{+} of positive s_{j} is binomial distributed with some mean $L\mu$ and variance $L\mu(1-\mu)$. Quantity μ is the proportion of positive s_{j} , which is related to the expectation value $E_{j}[s_{j}]$ via

$$\mu = \frac{\mathrm{E}_{j}[s_{j}] + 1}{2} \tag{9}$$

This equation simply transforms between the range $\mu \in [0, 1]$ and the range $E_j[s_j] \in [-1, +1]$, where, e.g., $\mu = 0 \Leftrightarrow E_j[s_j] = -1$ mean that none of the s_j is equal to +1, $\mu = 0.5 \Leftrightarrow E_j[s_j] = 0$ mean that half of the s_j are equal to +1, and $\mu = 1 \Leftrightarrow E_j[s_j] = 1$ mean that all s_j are equal to +1.

Since n_j^+ is binomial distributed, so is $\Sigma_j s_j$; and since the range [-L, L] of $\Sigma_j s_j$ has twice the range [0, L] of n_j^+ , the variance of $\Sigma_j s_j$ is four times that of n_j^+ . Using eq. (9), the variance thus is

$$\operatorname{var}_{j} \left[\sum_{j} s_{j} \right] = 4L\mu(1-\mu) = L\left(1 - \left(E_{j}[s_{j}]\right)^{2}\right), \tag{10}$$

and altogether

135

140

145

155

$$U_i(s_i) = (h + \sigma \varepsilon_i) s_i + (J_0 + s_i \Delta) s_i \mathcal{E}_j[s_j] - \rho \frac{(J_0 + s_i \Delta)^2}{L} s_i^2 \left(1 - \left(\mathcal{E}_j[s_j] \right)^2 \right). \tag{11}$$

Assuming rational individuals that maximise their risk utility, action $s_i = 1$ is chosen if and only if

$$\Delta U_{i} = U_{i}(s_{i} = +1) - U_{i}(s_{i} = -1) = 2(h + \sigma \varepsilon_{i}) + 2J_{0}E_{j}[s_{j}] - 4\frac{\rho J_{0}\Delta}{L} \left(1 - \left(E_{j}[s_{j}]\right)^{2}\right) > 0$$
(12)

Again following Phan et al. (2003) [27], I assume that the ε_i are logistically distributed according to

$$\Pr(\varepsilon_i \le z) = \frac{1}{1 + \exp\{-kz\}}$$
(13)

which for $k = \pi/3^{1/2}$ is very close to the normal distribution with mean zero and standard deviation one. Thus, the probability of individual *i* choosing $s_i = 1$ is

$$\Pr(s_i = 1) = \frac{1}{1 + \exp\{-\beta \Delta U_i\}}, \quad \beta = \frac{\pi}{3^{1/2} \sigma}$$
(14)

and the expectation value of s_i is

170

175

180

185

$$E[s_{i}] = \Pr(s_{i} = +1) - \Pr(s_{i} = -1)$$

$$= \frac{1}{1 + \exp\{-\beta \Delta U_{i}\}} - \left(1 - \frac{1}{1 + \exp\{-\beta \Delta U_{i}\}}\right) = \tanh\{-\beta \Delta U_{i} / 2\}$$
(15)

Using the classical mean-field approximation, all individuals have the same payoffs h, J and Δ , so the expectation $E[s_i]$ and $E_i[s_i]$ are identical and the same for all i, so that finally

$$m = E[s] = f(m)$$
with $f(m) = \tanh \{\beta \Delta U / 2\} = \tanh \left\{\beta \left(h + J_0 m - 2\frac{\rho J_0 \Delta}{L} (1 - m^2)\right)\right\}$
(16)

For $\rho = 0$, eq. (16) represents the well-known self-consistency equation for the magnetisation in the ferromagnet, while risk aversion, $\rho > 0$ reduces the argument in the tanh function. However, risk aversion has only an effect if the risk difference Δ is non-zero. The effect of risk aversion further diminishes with the size L of the neighbourhood, because the larger the neighbourhood the more the variation in the s_j cancels out (equivalent to the central limit theorem). And the effect of risk aversion is strongest for m close to zero because here the variation in the s_i (eq. 10) is highest.

Equation (16) is solved systematically for various combinations of βJ_0 and $\beta \rho \Delta / L$ to explore the impacts of the coupling constant J_0 and the risk term, $\rho \Delta / L$. A change in β is equivalent to a

reciprocal change in J_0 and $\rho\Delta/L$, and is thus not analysed explicitly. The "external field" h whose effect is the same as in the classical Ising model of the ferromagnet is set to zero to focus on the joint impacts of coupling constant and risk aversion.

190

2.2 Results

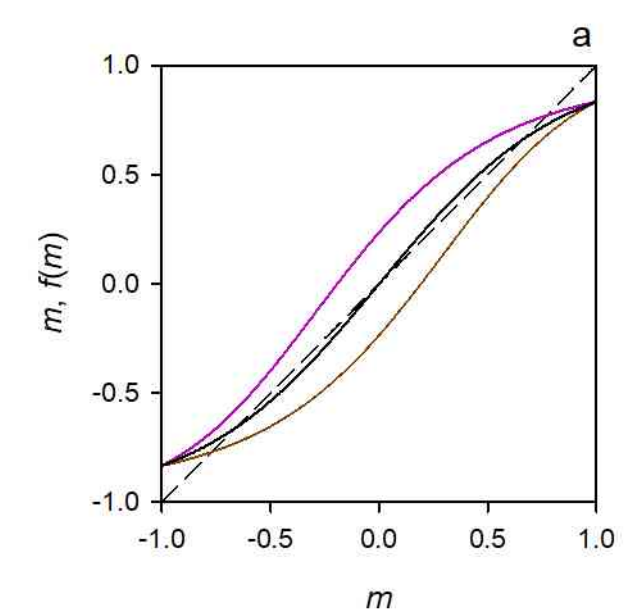
Figure 1a shows the main effect of the risk term $\rho\Delta/L$. For the ferromagnet, $\rho\Delta/L = 0$, eq. (16) has (for h = 0) a single solution $m^* = 0$ if $\beta J_0 \le 1$, and otherwise a positive and a negative solution (the zero solution becomes unstable) both of equal magnitude. The solid line in Fig. 1a shows these two solutions for $\beta J_0 = 1.2$. If $\beta \rho\Delta/L$ is increased to 0.1, f(m) is represented by the purple line, showing that the positive solution disappears and the negative solution slightly increases in magnitude. A reduction to $\beta \rho\Delta/L = -0.1$ (brown line) leads to the "opposite" result that the positive solution slightly increases in magnitude and the negative solution disappears (which is readily explained by the symmetry of eq. (16) with respect to the joint transformation $s_i \to -s_i$ and $\Delta \to -\Delta$).

200

205

195

The disappearance of the positive or negative solution is discontinuous so that its magnitude does not decline continuously to zero. The same is observed for the influence of βJ_0 for given $\beta \rho \Delta / L$. For illustration, consider the brown line in Figure 1b which corresponds to the brown line in Fig. 1a (βJ_0 = 1.2 and $\beta \rho \Delta / L = 0.1$). Increasing βJ_0 yields no positive solution until at a value of about 1.45 (orange line in Fig. 1b) a positive solution of $m^* \approx 0.7$ appears. The value $\beta J_0 = 1.4$ is thus a critical value below which no positive solution exists and above which the it emerges and increases monotonously with further increasing βJ_0 (purple line in Fig. 1b).



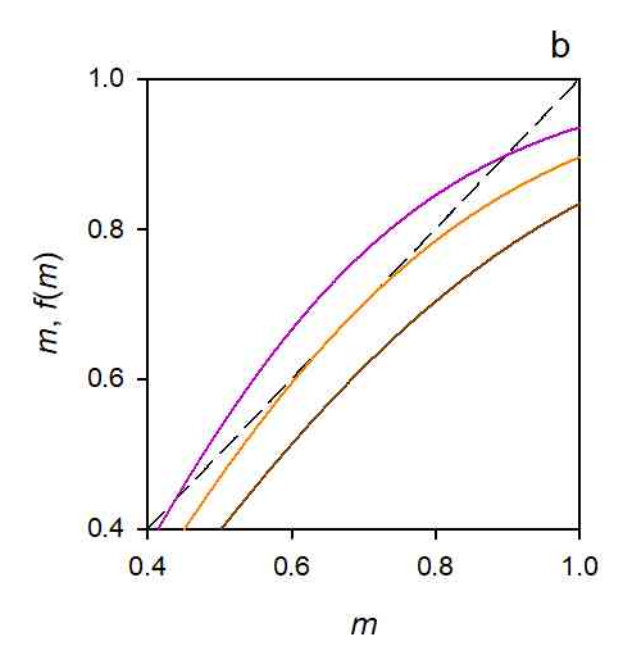


Figure 1: Left-hand side (m: dashed line) and right-hand side (f(m): other lines) of eq. (16) as functions of m. In panel a the coupling constant is $\beta J_0 = 1.2$ and the black solid line represents $\beta \rho \Delta / L = 0$, while the purple and brown lines represent $\beta \rho \Delta / L = +0.1$ and -0.1, respectively. In panel b the risk term is $\beta \rho \Delta / L = +0.1$ and coloured lines represent, from bottom to top, $\beta J_0 = 1.2$, 1.45 and 1.7, respectively.

The dependence of the positive and the negative solutions on βJ_0 and $\rho \Delta/L$ is shown comprehensively in Fig. 2. First focus on the right halves, $\rho \Delta > 0$, of the two panels. Two solutions, a positive and a negative one, are obtained only for sufficiently large βJ_0 above some critical $(\beta J_0)_c$ whose magnitude increases in a concave manner with increasing $\beta \rho |\Delta|/L$; while for smaller βJ_0 only a single (negative for $\Delta > 0$ and positive for $\Delta < 0$) solution exists. Statistical regression estimates the phase boundary between the two regions in parameter space to

$$(\beta J_0)_c \approx 1 + \exp(1/4) \left(\frac{2\beta\rho |\Delta|}{L}\right)^{2/3}$$
(17)

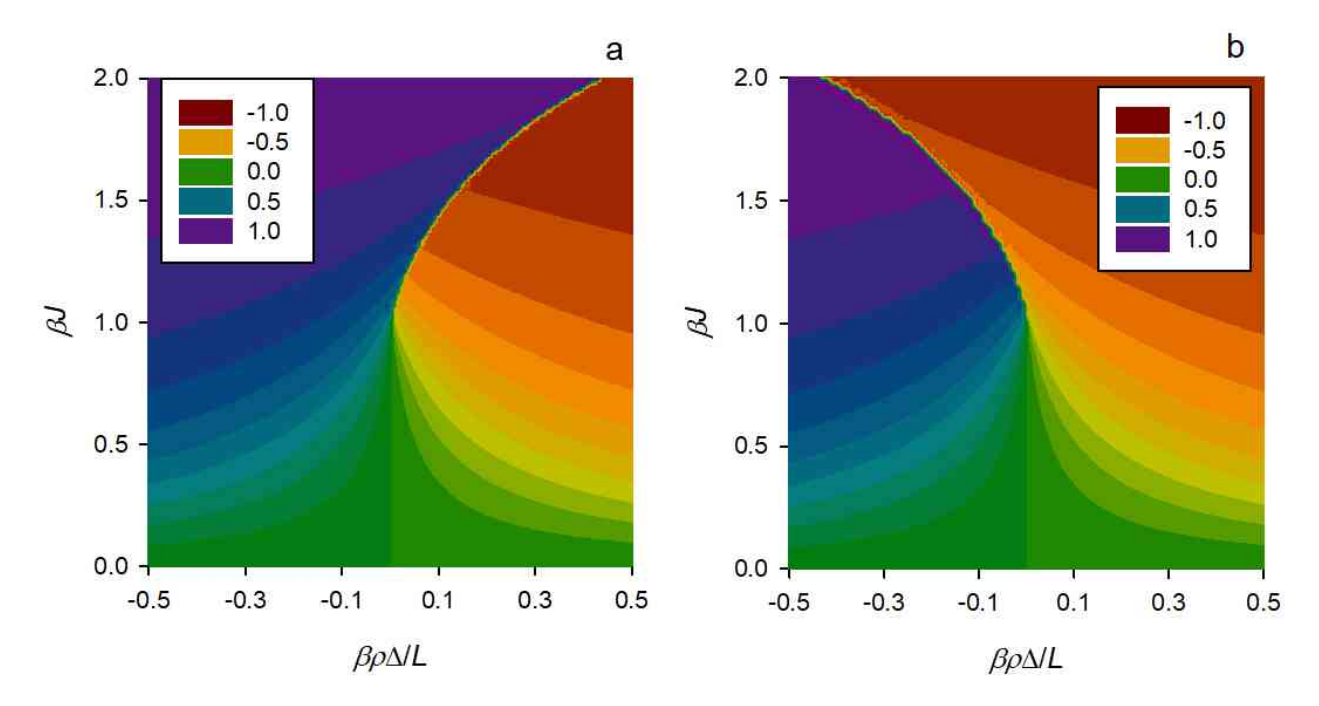


Figure 2: Solution of eq. (16) as a function of the coupling constant βJ_0 and the risk coefficient $\beta \rho \Delta / L$ by continuous colour scale. The colour legend shows five selected colours and associated levels of m^* . Where both panels show the same value only a single solution exists; where the values differ, panel a shows the larger of the two (which is the positive solution) and panel b shows the smaller of the two (which is the negative solution).

230

215

In the following I will consider only the positive solution, where it exists (Fig. 2a). For $\rho\Delta > 0$ (area above the phase boundary in Fig. 2a), its magnitude increases with increasing βJ_0 and decreases with increasing $\beta \rho\Delta/L$; while for $\rho\Delta < 0$ (left half of Fig. 2a) it increases with increasing βJ_0 and increasing $\beta \rho|\Delta|/L$.

235

240

245

The behaviour of the positive solution m^* above the phase boundary, $\beta J_0 > (\beta J_0)_c$ can be seen more clearly in Fig. 3a. The lines represent vertical cross-section through the contours in Fig. 1a above the phase boundary, showing the dependence of m^* as a function of βJ_0 , with $\beta J_0 > (\beta J_0)_c$ and $(\beta J_0)_c$ defined above.

First consider the "starting points" of the lines. As demonstrated in Fig. 1b, a positive m^* does not exist for $\beta J_0 \le (\beta J_0)_c$, but emerges when βJ_0 crosses $(\beta J_0)_c$. As Fig. 3a shows, the "critical" level m^*_c , i.e. the level of m^* that emerges when βJ_0 crosses $(\beta J_0)_c$, depends on $(\beta J_0)_c$ of eq. (17). Statistical regression of the numerical results relates m^*_c to $(\beta J_0)_c$ quite precisely via

$$m_{c}^{*} = ((\beta J_{0})_{c} - 1)^{1/2}$$
(18)

which is represented by the dashed line in Fig. 3a. Having estimated m^*_c as a function of $(\beta J_0)_c$ and $(\beta J_0)_c$ as a function of $\beta \rho \Delta L$, turn to the behaviour of m^* when βJ_0 increases beyond $(\beta J_0)_c$. Plotting the solid lines in Fig. 3a in log-log scale leads to straight lines with slopes of about 0.5, so that

$$m^* - m^*_{c} \sim (\beta J_0 - (\beta J_0)_{c})^{1/2}$$
 (19)

Alternatively, one could relate $m^* - m^*_c$ to $1 - (\beta J_0)_c/(\beta J_0)$. Figure 3b relates these two quantities in log-log scale, also obtaining straight lines with some slope k, so that

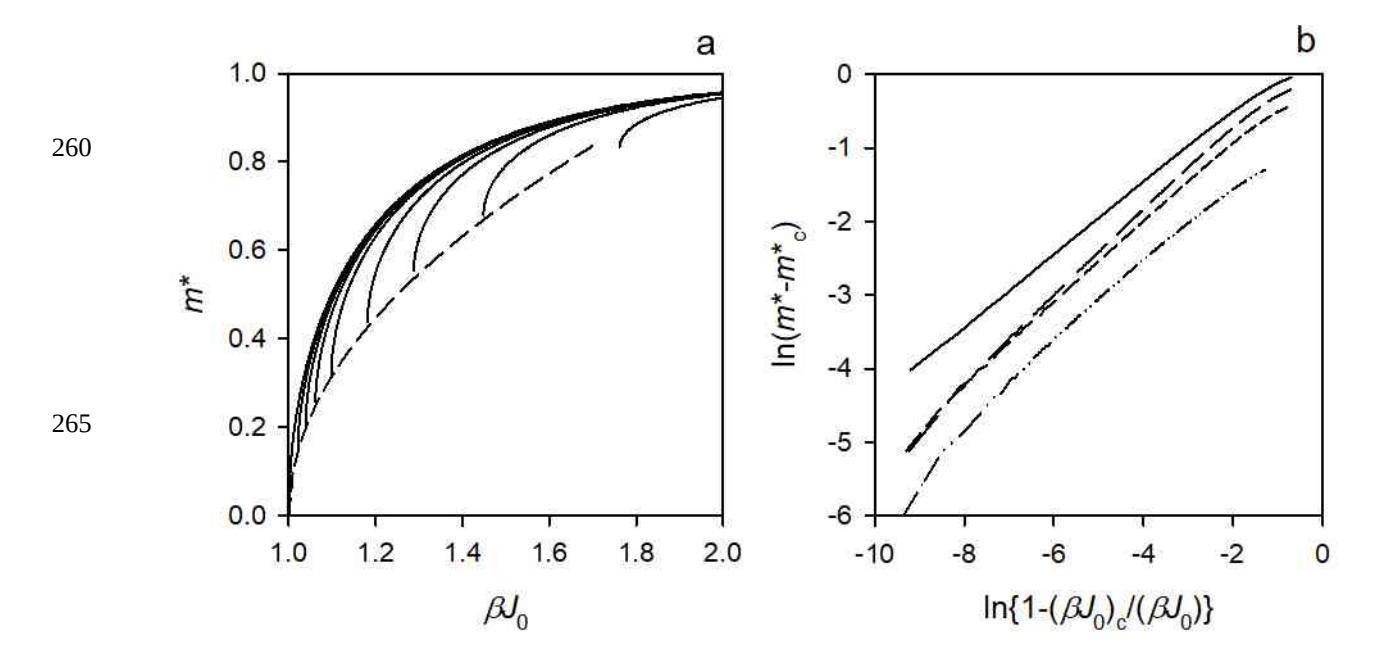


Figure 3: Details of the model behaviour. Panel a shows the positive solution of eq. (16) m^* as a function of βJ_0 for various levels of $\beta \rho \Delta / L \ge 0$ ($\beta \rho \Delta / L$ increasing from the lower right to the upper left with levels 0, 0.001, 0.0025, 0.005, 0.01, 0.025, 0.05, 0.1, 0.25). The dashed line marks the minimum of m^* as a function of $(\beta J_0)_c$, where $(\beta J_0)_c$ is the critical level of (βJ_0) below which no positive solution m^* exists. Panel b shows the dependence of m^* on βJ_0 in log-log scale (further explanations in the text). The solid line here represents $\beta \rho \Delta / L = 0$ and the other lines represent, from top to bottom, $\beta \rho \Delta / L = 0.001$, 0.01 and 0.1.

$$m^* - m^*_{c} \sim \left(1 - \frac{(\beta J_0)_{c}}{\beta J_0}\right)^k$$
 (20)

For $\beta\rho\Delta/L=0$ the line slope is about $k\approx0.5$, as in eq. (19), and for the considered non-zero levels of $\beta\rho\Delta/L$ the slope is $k\approx5/8$. Fixing J_0 at some particular level and identifying β as the inverse of the temperature T of the spin system [27] (Phan et al. 2003), the term in parentheses in eq. (19) is the relative deviation $1-T/T_c$ of the temperature from its critical value $T_c\equiv1/\beta_c$. Exponent k is thus the critical exponent that relates the order parameter of the spin system to the system temperature. For the Ising model of the ferromagnet this value is known [29] to be 0.5 (e.g., Utermohlen 2018); the value of about 5/8 obtained for non-zero $\beta\rho\Delta/N$ indicates a slight change of the system's critical behaviour.

Lastly, turn to the model behaviour for $\beta \rho \Delta / L < 0$ (left half of Fig. 2a). There are no discontinuities in m^* as a function of βJ_0 (Fig. 4), but with increasing $\beta \rho |\Delta| / L$ the lines increasingly and smoothly

deviate from the square-root shape obtained for $\beta \rho \Delta / L = 0$, so that at larger $\beta \rho |\Delta| / L$ a sigmoid dependence of m^* on βJ_0 is observed.

295

300

*E 0.4 - 0.2 - 0.0 0.5 1.0 1.5 2.0

305

Figure 4: Positive solution m^* of eq. (16) as a function of βJ_0 for various levels of $\beta \rho \Delta / L \le 0$ ($\beta \rho \Delta / L$ decreasing from the lower left to the upper right with levels 0, -0.001, -0.01, -0.01).

3 Application: the agglomeration bonus

As described in Drechsler (2023) [24], under an agglomeration bonus scheme the conservation of a land parcel *i* earns a payment of size

$$p_i = p_0 + b \sum_{j \in L_i} x_j \tag{21}$$

where p_0 is a spatially homogenous base payment and the bonus b is paid for each conserved land parcel in the neighbourhood L_i (typically the von-Neumann neighbourhood of the four adjacent land parcels or the Moore neighbourhood of the eight adjacent land parcels).

Conservation of land parcel *i* also incurs a cost (e.g., forgone agricultural revenues)

$$c_i = c_0(1 - \sigma \varepsilon_i) \tag{22}$$

where ε_i is a normal distributed random number with mean zero and standard deviation one, and σ measures the spatial variation of the conservation costs in the model landscape. If conservation of land parcel i is represented by $x_i = 1$ and economic use by $x_i = 0$ the profit V_i on land parcel i is

$$V_i(x_i) = x_i \left(p_0 + b \sum_{j \in L_i} x_j \right) + c_0 (1 - \sigma \varepsilon_i) (1 - x_i)$$
(23)

With the transformation $s_i = 2(x_i - 1/2)$ this writes

 $V_{i}'(s_{i}) = \frac{1}{2} \left[(p_{0}' - 1 + \frac{b'L}{2} + \sigma\varepsilon_{i})s_{i} + \frac{b'}{2}(s_{i} + 1)\sum_{j \in L_{i}} s_{j} \right] + \text{const.}$ (24)

with dimensionless quantities $V_i' \equiv V_i/c_0$, $p_0' \equiv p_0/c_0$ and $b' \equiv b'/c_0$ (so all economic quantities are scaled relative to the mean conservation cost c_0), and where const. includes the terms independent of s_i and s_i .

Writing $s_i + 1 = s_i + s_i^2$ one obtains eq. (2) with

$$h = p_0 - 1 + \frac{b'L}{2}$$

$$J_0 = \Delta = b'/2 \qquad . \tag{25}$$

According to Fig. 2, the positivity of Δ implies that the expected value m^* of s_i declines with increasing disk aversion ρ . For a more practical understanding of the effect of ρ and an easier reference to the results of Drechsler (2023) [24], I return to eq. (23) and insert the risk aversion analogous to section 2 by calculating the variance of $V_i(x_i = 1)$ (since $V_i(x_i = 0)$ does not depend on the x_j in the neighbourhood of land parcel i, its variance is zero):

$$\operatorname{var}_{j}[V_{i}(x_{i}=1)] = b^{2} \operatorname{var}_{j}\left[\sum_{j \in L_{i}} x_{j}\right] = L\mu(1-\mu),$$
(26)

with $\mu = E[x_i] = Pr(x_i)$. Combining with eq. (24), the risk utility of landowner *i* becomes

325

330

335

340

$$U_{i}'(x_{i}) = \begin{cases} p_{0}' + b' L \mu - \rho b'^{2} L \mu (1 - \mu) & x_{i} = 1\\ 1 - \varepsilon_{i} & x_{i} = 0 \end{cases}$$
(27)

With eq. (13), and analogous to eq. (14), I obtain

$$\mu = f(\mu) = \frac{1}{1 + \exp\left\{-\beta \left(p_0' - 1 + b' L \mu - \rho b'^2 L \mu (1 - \mu)\right)\right\}}.$$
(28)

To derive a meaningful upper bound on ρ , consider that the payoff p_0 ' is certain, so that U_i '(1) cannot be smaller than p_0 '; meaning that the risky part of the payoff from the bonus, $\rho b'^2 L \mu (1 - \mu)$, cannot be larger than the expectation part, $b'L\mu$. Considering an upper bound on b' of 20 (which well encompasses values in real conservation payment schemes [24]: Drechsler (2023)), this requirement is fulfilled for all $\mu \in [0, 1]$ if $\rho \le 0.05$.

As already discussed by Drechsler (2023) [24], eq. (28) has either a single or two stable solutions μ^* , shown in the upper and lower panels of Fig. 5, respectively. Comparing the panels reveals that increasing risk aversion leads to more parameter combinations with bistability, especially at large bonuses b where the single solution with large μ^* is accompanied by a solution with small μ^* .

4 Discussion

360

365

370

375

Ising models are increasingly used for the description of biological and social systems in which interactions between individuals plays a role. In contrast to physical entities like magnetic spins, living individuals often exhibit more complex decision behaviour and reaction to other individuals' decisions. An important one that is considered here is attitude towards risk and uncertainty; and in particular that humans and many animals are usually averse to risk and, next to the maximisation of expected payoffs aim at the minimisation of risk. This is reflected in the applied mean-variance criterion [28] (Nakamura 2015) in which the variance of the payoff, multiplied by some risk-attitude factor ρ (> 0 for risk aversion), is subtracted from the expected payoff. In the present paper I integrated this decision model into the classical Ising model and analysed the model using the mean field approach by Phan et al. (2003) [27].

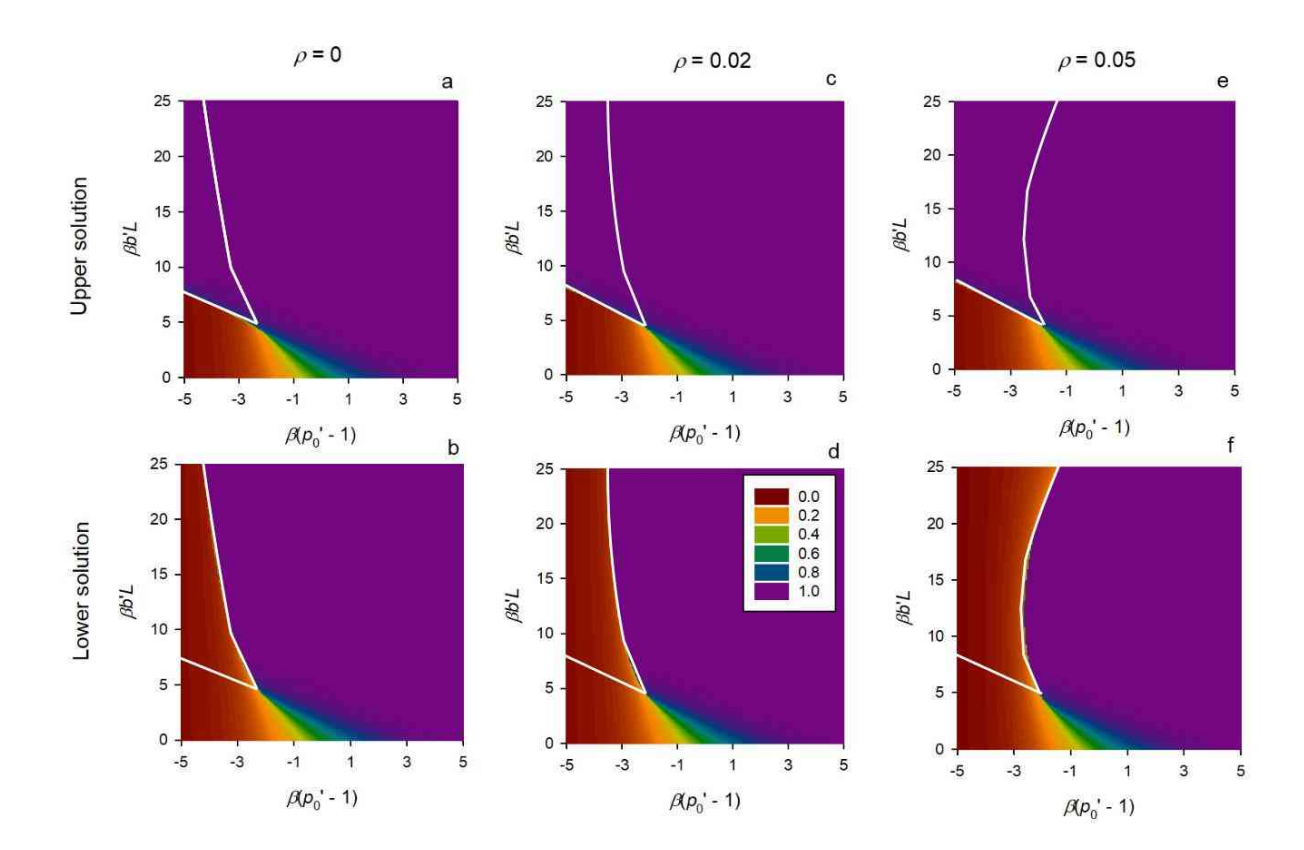


Figure 5: Equilibrium proportion (as the solution of eq. (28)) of conserved land parcels μ^* , by continuous colour scale from zero to one, as a function of the scaled base payment $\beta(p_0'-1)$ and the scaled bonus $\beta b'L$. The colour legend shows six selected colours and associated levels of μ^* . If there is only a single solution μ^* it is shown in both panels; if there are two solutions the upper one is showing in the respective upper panel and the lower solution in the lower panel. Risk aversion increases from left to right with $\rho = 0$, 0.01 and 0.05.

390

395

385

As a first result it turns out that risk aversion has only an effect if the magnitude of the risk differs between the two choices available to an individual in an Ising model, described by the parameter Δ in eq. (2). Technically this was considered here by depending the coupling constant on the value (+1 or -1) of the "spin" s_i . Not very unexpected, the equilibrium proportion of individuals choosing a particular s_i is reduced if the risk associated with that s_i is larger than that associated with the opposite s_i (indicated in Fig. 2a by the size of the positive solution, $m^* > 0$, declining with increasing risk difference $\Delta > 0$).

Increasing the product of risk difference Δ and risk aversion ρ raises the critical level βJ_c of the coupling constant J (with β the inverse temperature or inverse spatial heterogeneity in the individuals' idiosyncratic payoffs). If $\rho \Delta > 0$, for $\beta J > \beta J_c$ the m^* depends on the difference $\beta J - \beta J_c$ in a very similar manner as it depends on βJ if $\rho \Delta = 0$. If βJ falls below βJ_c (or $\rho \Delta$ increases so that βJ_c exceeds a given βJ) the positive solution $m^* > 0$ disappears.

An intuitive understanding of these results can be obtained from the application considered in section 3. Here the decision to conserve a piece of land for biodiversity is rewarded by a payment *p* that consists of a guaranteed base payment and a bonus for each conserved land parcel in the neighbourhood. The latter is uncertain to the focal landowner – in contrast to the payoff from economic use (e.g., agricultural profit) which is certain. If the base payment is rather small and the bonus rather large the total payment *p* exceeds the economic payoff when all or many neighbours conserve but falls short if none or only few neighbours conserve. Here the landowner has to decide whether to choose the "payoff-dominant" strategy of conserving, or the "risk-dominant" strategy of economic use. On the regional scale of multiple landowners this reflects in payoff and risk-dominant Nash equilibria [25, 30] (Parkhurst et al 2002, Parkhurst and Shogren 2007) and the bistability observed in the present analysis.

This bistability where the land-use system is either in a state of much conservation or in a state of little conservation is observed even for risk-neutral landowners, $\rho = 0$ (Fig. 5a,b). Increasing risk aversion, however, makes the landowners more sensitive to the risk difference, so that especially at large levels of the bonus the range of base payments that leads to bistability expands (Figs. 5c–f). Risk averse landowners are thus less inclined to choose the payoff-dominant conservation use f the risk difference between conservation and economic use (bonus $\sim \Delta$) is large.

From a conservation-practical point of view, one may ask how this risk can be mediated and the landowners induced into conservation at a large scale. Experimental research on the agglomeration bonus [30–33] (Parkhurst and Shogren 2007, Banerjee et al. 2014, 2016, 2018) highlights the importance of information provision and communication between the landowners. Future research may explore how these factors affect the performance of the agglomeration bonus in particular, and the economic or social dynamics of interacting individuals in general.

References

400

420

425

430

[1] K.H. Fischer, J.A. Hertz, Spin Glasses, Cambridge University Press, 1991.

- [2] Y.-P. Ma. I. Sudakov. C. Strong, K. Golden, Ising model for melt ponds on Arctic sea ice. New J.Phys. 21 (2017), 063029.
 - [3] E.T. Jaynes, (1957), Information Theory and Statistical Mechanics. Phys. Rev. 106(4) (1957), 620–630.
- [4] B. Derrida, E. Gardner, A. Zippelius, An exactly solvable asymmetric neural network model. Europhys. Lett. 4(2) (1987), 167–173.
 - [5] M. Krasnytska, B. Berche, Y. Holovatch, R. Kenna, Generalized Ising model on a scale-free network: an interplay of power laws. Entropy 23 (2021), 1175.
 - [6] Y. Shi, T. Duke, Cooperative model of bacteril sensing. Phys. Rev. E. 58(5) (1998), 6399–6406.
- [7] F. Bai, R.W. Branch, D.V. Nicolau, T. Pilizota, B.C. Steel, P.K. Maini, R.M. Berry,
 Conformational Spread as a Mechanism for Cooperativity in the Bacterial Flagellar Switch. Science
 327 (2010), 685–689.
 - [8] J. Majewski, H. Li, J. Ott, The Ising model in physics and statistical genetics. Am. J. Hum. Genet. 69 (2001), 853–862.
- 455 [9] T.C. Schelling, Models of segregation. Am. Econ. Rev. 59 (1969), 488–93.

445

- [10] D. Stauffer. Social applications of two-dimensional Ising models. Am. J. Phys. 76 (2008), 470.
- [11] A.Grabowski, R.A.Kosiński, Ising-based model of opinion formation in a complex network of interpersonal interactions, Physica A: Statistical Mechanics and its Applications 361(2) (2006), 651–664.
 - [12] M. Garrod, N.S. Jones, Influencing dynamics on social networks without knowledge of network microstructure. J. R. Soc. Interface 18 (2021), 20210435.
 - [13] M. Valle, J.F. Lavín, N.S. Magner, Equity Market Description under High and Low Volatility Regimes Using Maximum Entropy Pairwise Distribution. Entropy 23 (2021), 1307.

- [14] K. Bhattacharya, T. Vicsek, Collective decision making in cohesive flocks. New J. Phys. 12470 (2010), 093019.
 - [15] S.P. Wilson, Modelling the emergence of rodent filial huddling from physiological huddling. J. R. Soc. Open sci. 4 (2017), 170885.
- [16] V. Lecheval, J. Li, P. Tichit, C. Sire, C.K. Hemelrijk, G. Theraulaz, Social conformity and propagation of information in collective U-turns of fish schools. Proc. R. Soc. B. 285 (2018), 20180251.
- [17] L. Eeckhoudt, H. Schlesinger, C. Gollier, Economic and Financial Decisions Under Risk,Princeton University Press (2005).
 - [18] J.M. Chen, Risk Aversion, in: Finance and the Behavioral Prospect. Quantitative Perspectives on Behavioral Economics and Finance. Palgrave Macmillan (2016).
- [19] A. Batabyal, S. Balakrishna, M. Thaker, A multivariate approach to understanding shifts in escape strategies of urban lizards, Behav. Ecol. Sociobiol. 71 (2017), 83.
 - [20] C.M. Constantinople, A.T. Piet, C.D. Brody, An Analysis of Decision under Risk in Rats. Curr. Biol. 29 (2019), 2066–2074.

- [21] E.O.C. Coni, D.J. Booth, I. Nagelkerken, Coral-reef fishes can become more risk-averse at their poleward range limits. roc. R. Soc. B. 289 (2022), 20212676.
- [22] W.D. Clayton, S.M. Brantley, T.T. Zentall, Decision making under risk: framing effects in pigeon risk preferences. Anim. Cogn. 25 (2022), 1281–1288.
 - [23] L.M., Haux, J.M. Engelmann, R.C. Arslan, R. Hertwig, E. Herrmann, Chimpanzee and human risk preferences show key similarities. Psychol. Sci. 34(3) (2023), 358–369.
- 500 [24] M. Drechsler, Insights from Ising models of land-use under economic coordination incentives. Physica A (2023) in press.

[25] G.M. Parkhurst, J.F. Shogren, C. Bastian, P. Kivi, J. Donner, R.B.W. Smith, 2002. Agglomeration bonus: An incentive mechanism to reunite fragmented habitat for biodiversity conservation. Ecol. Econ. 41 (2002), 305–328.

505

510

520

- [26] C. Nguyen, U. Latacz-Lohmann, N. Hanley, S. Schilizzi, S. Iftekhar, Coordination Incentives for landscape-scale environmental management: A systematic review, Land Use Policy 114 (2022) 105936.
- [27] D. Phan, M.B. Gordon, J.-P. Nadal, Social interactions in economic theory: an insight from Statistical Mechanics, in: P. Bourgine, J.-P. Nadal, J.-P. (eds.), Cognitive Economics, Springer (2003), pp. 333–356.
- 515 [28] Y. Nakamura. Mean-variance utility. Int. J. Econ. Theory 160 (2015) 536–556.
 - [29] F. Utermohlen, Mean Field Theory Solution of the Ising Model. https://bpb-us-w2.wpmucdn.com/u.osu.edu/dist/3/67057/files/2018/09/Ising_model_MFT-25b1klj.pdf (last access 07/07/2023).
 - [30] G.M. Parkhurst, J.F. Shogren, Spatial incentives to coordinate contiguous habitat. Ecol. Econ. 64 (2007), 344–355.
- [31] S. Banerjee, A.M. Kwasnica, J.S. Shortle, Agglomeration bonus in small and large local networks: A laboratory examination of spatial coordination. Ecol. Econ. 84 (2012), 142–152.
 - [32] S. Banerjee, T.N. Cason, F.P. de Vries, N. Hanley, Transaction costs, communication and spatial coordination in Payment for Ecosystem Services schemes. J. Environ. Econ. Manage. 87 (2016), 68–89.
 - [33] L. Kuhfuss, R. Préget, S. Thoyer, F.P. de Vries, N. Hanley, Enhancing spatial coordination in payment for ecosystem services schemes with non-pecuniary preferences. Ecol. Econ. 192 (2022), 107271.